



Strnadel, J. et al. (2018) Survival of syngeneic and allogeneic iPSC–derived neural precursors after spinal grafting in minipigs. *Science Translational Medicine*, 10(440), eaam6651. (doi:[10.1126/scitranslmed.aam6651](https://doi.org/10.1126/scitranslmed.aam6651))

This is the author’s final accepted version.

There may be differences between this version and the published version. You are advised to consult the publisher’s version if you wish to cite from it.

<http://eprints.gla.ac.uk/162268/>

Deposited on: 15 May 2018

Enlighten – Research publications by members of the University of Glasgow

<http://eprints.gla.ac.uk>

Survival of syngeneic and allogeneic iPSCs-derived neural precursors after spinal grafting in minipigs.

^{1,2}Jan Strnadel, ³Cassiano Carromeu, ^{4,5}Cedric Bardy, ¹Michael Navarro, ¹Oleksandr Platoshyn, ¹Andreas N. Glud, ¹Silvia Marsala, ¹Jozef Kafka, ^{1,6}Atsushi Miyano-hara, ⁷Tomohisa Kato Jr., ¹Takahiro Tadokoro, ¹Michael Hefferan, ¹Kota Kamizato, ¹Tetsuya Yoshizumi, ⁸Stefan Juhas, ⁸Jana Juhasova, ⁹Chak-Sum Ho, ⁹Taba Kheradmand, ¹PeiXi Chen, ^{1,10}Dasa Bohaciakova, ^{1,11}Marian Hruska-Plochan, ¹²Andrew J. Todd, ¹³Shawn P. Driscoll, ¹³Thomas D. Glenn, ¹³Samuel L. Pfaff, ⁸Jiri Klima, ¹⁴Joseph Ciacci, ¹⁴Eric Curtis, ⁴Fred H. Gage, ¹⁵Jack Bui, ¹⁶Kazuhiko Yamada, ³Alysson Muotri, ^{1,17}Martin Marsala

¹Neuroregeneration Laboratory, Department of Anesthesiology,

University of California-San Diego (UCSD), La Jolla, CA, 92037, USA;

²Biomedical Center Martin, Department of Molecular Medicine, Jessenius Faculty of Medicine in Martin, Comenius University in Bratislava, 03601 Martin, Slovakia;

³Department of Pediatrics, UCSD;

⁴Laboratory of Genetics, The Salk Institute for Biological Studies, La Jolla, CA, 92037, USA;

⁵Laboratory for Human Neurophysiology and Genetics, SAHMRI Mind and Brain, Australia;

⁶Vector Core Laboratory, UCSD;

⁷Center for iPS Cell Research and Application (CiRA), Kyoto University, Japan;

⁸Institute of Animal Physiology and Genetics, v.v.i., AS CR, Liběchov, Czech Republic;

⁹Histocompatibility Laboratory, Gift of Life Michigan, Ann Arbor, MI, 48108, USA;

¹⁰Department of Histology and Embryology, Masaryk University, Brno, Czech Republic;

¹¹Institute of Molecular Life Sciences, University of Zurich, Winterthurerstrasse 190, 8057 Zurich, Switzerland;

¹²Institute of Neuroscience and Psychology, College of Medical,

Veterinary and Life Sciences, University of Glasgow, Glasgow G12 8QQ, UK;

¹³Gene Expression Laboratory and the Howard Hughes Medical Institute, Salk Institute for Biological Studies, La Jolla, CA, 92037, USA;

¹⁴Department of Neurosurgery, UCSD;

¹⁵Department of Pathology, UCSD;

¹⁶Columbia University Medical Center Campus, NY, 10032, USA;

¹⁷Institute of Neurobiology, Slovak Academy Of Sciences, Kosice, Slovakia

One sentence summary: Syngeneic iPSCs-derived neurons survive and mature without immunosuppression after grafting into spinal cord of adult pig.

Correspondence:

Martin Marsala, M.D.

University of California, San Diego

Neuroregeneration Laboratory

Department of Anesthesiology

SCRM, Room 4009

2880 Torrey Pines Scenic Dr.

La Jolla, CA 92037

e-mail: mmarsala@ucsd.edu

Ph (office): 858-822-3805

Ph (lab): 858-534-7380

Fax: 858-822-3249

Abstract

The use of autologous (or syngeneic) cells derived from induced pluripotent stem cells (iPSCs) holds great promise for future clinical use in a wide range of diseases and injuries. It is expected that cell replacement therapies using autologous cells would forego the need for immunosuppression, otherwise required in allogeneic transplantations. However, recent studies have shown the unexpected immune-rejection of undifferentiated autologous mouse iPSCs after transplantation. Whether similar immunogenic properties are maintained in iPSCs-derived lineage-committed cells (such as neural precursors) is relatively unknown. Here we demonstrate that syngeneic porcine iPSCs-derived neural precursor cells (NPCs) transplantation to the spinal cord in absence of immunosuppression is associated with long-term survival and neuronal and glial differentiation. No tumor formation was noted. Similar cell engraftment and differentiation was shown in spinally-injured transiently immunosuppressed swine leukocyte antigen (SLA)-mismatched allogeneic pigs. These data demonstrate that iPSCs-derived NPCs can be grafted into syngeneic recipients in the absence of immunosuppression and that temporary immunosuppression is sufficient to induce long-term immune tolerance after NPCs engraftment into spinally-injured allogeneic recipients. Collectively, our results show that iPSCs-NPCs represent an alternative source of transplantable NPCs for the treatment of a variety of disorders affecting the spinal cord including trauma, ischemia or amyotrophic lateral sclerosis.

INTRODUCTION

The technology for generating iPSCs (1, 2) has opened new possibilities for patient-specific cell therapy, in vitro disease modeling and drug discovery. Although disease-specific iPSCs provide an excellent tool for studying the developmental pathology of human diseases in vitro (3, 4), the use of iPSCs for spinal cord autologous, syngeneic or allogeneic transplantation has never been tested in large animal models. The use of large animal models that show similarities in spinal cord and CNS anatomy and function with humans are necessary for advancing cell transplantation therapies using iPSCs technology to a clinical setting.

Given the ethical issues related to the use of primates, pigs serve as an alternative model for preclinical experiments in regenerative medicine (5, 6). However, isolation of embryonic stem cells (ESCs) from pigs is difficult and not effective (7). Several groups reported successful generation of pig iPSCs, but the engraftment properties of autologous or syngeneic iPSCs-derived neural precursors once grafted back into CNS were rarely explored (8-11). Therefore, we sought to test the immunogenicity and engraftment properties of iPSCs-derived lineage-committed NPCs, which are expected to be free of pluripotent cell contaminants and therefore not form teratoma-like tumor masses.

Here, we analyze syngeneic transplantations of pig NPCs derived from SLA-inbred pig iPSCs. NPCs were isolated by manual clone selection, expanded and characterized before transplantation. Three months after transplantation into the spinal cord of syngeneic recipients in the absence of immunosuppression, NPCs showed robust engraftment and neuronal/glia differentiation without detectable rejection or tumor formation. In addition, a comparable degree of cell engraftment and differentiation was observed after allogeneic transplant in transiently immunosuppressed pigs with previous chronic spinal traumatic injury. No detectable presence of circulating anti-iPSCs-NPCs antibodies was seen in iPSCs-NPCs-grafted non-immunosuppressed syngeneic or transiently-immunosuppressed allogeneic pigs.

These data demonstrate the lack of immunogenicity of iPSCs-NPCs engrafted into naive non-injured or spinal trauma-injured spinal cord. In addition, the successful engraftment observed in allogeneic animals receiving only time-limited immunosuppression indicates a potential for clinical utilization of human iPSCs-derived NPCs in patients with a different human leukocyte antigen signature.

RESULTS

NPCs derived from reprogrammed adult porcine skin fibroblasts generate functional neurons in vitro

We first generated the porcine iPSCs-derived NPCs. Four fully SLA-matched adult pigs were used to obtain skin biopsies (**Fig. 1A**). All tissue explants successfully produced fibroblasts (**Fig. 1B**) and pluripotent colonies (**Fig. 1 C, D**) after reprogramming using Sendai vectors (12) encoding octamer-binding transcription factor 4 (*OCT4*), (sex determining region Y)-box 2 (*SOX2*), Kruppel-like factor 4 (*KLF4*) and myelocytomatosis viral oncogene (*c-MYC*). Expression of the pluripotent markers such as *KLF4*, *SOX2*, *OCT4* and Nanog homeobox (*NANOG*) was seen in proliferating iPSCs colonies (**Fig. 1 E-H**). Previously frozen iPSCs (passage 12-18) showed a comparable formation of pluripotent colonies and expression of pluripotent markers (**fig. S1 A-F**).

To test the differentiation potential of established iPSCs three different in vitro or in vivo assays were used. First, proliferating colonies were induced to form embryoid bodies (EBs) (**Fig. 1I**) and continuously cultured in the presence of pig serum (0.1-1%) for 3-4 weeks. Second, a single monolayer of iPSCs was induced using established germ layer-specific (ectoderm, endoderm or mesoderm) induction protocols for 10-14 days. After induction, EBs and induced iPSCs were stained with markers of mesoderm [smooth muscle actin-SMA, Brachyury), endoderm (alpha-fetoprotein (AFP), sex determining region Y (*SOX17*)] and ectoderm [orthodenticle homeobox 2 (*OTX2*), neuron-specific Class III β -tubulin (*TUJ1*)]. Third, a single cell suspension of iPSCs was injected into the testes of immunodeficient mice and the presence of teratomas analyzed at 4-8 weeks after injection. Staining of in vitro-induced EBs (**fig. S1 G-J**) or induced single cell-seeded iPSCs (**fig. S1 K-M**) shows the expression of definitive ectoderm, endoderm and mesoderm markers. Macroscopic inspection of iPSCs-injected testes showed extensive bilateral tumor formation at intervals longer than 5 weeks after cell injection (**fig. S1 N-left bottom black-background inset**). H&E staining of histological sections taken from injected testes showed developed teratomas with all 3 germ layer derivatives (**Fig. 1J and fig. S 1N**).

To generate NPCs, EBs were cultured in the presence of basic fibroblast growth factor (bFGF) to potentiate the formation of neural rosettes (**Fig. 1K**). Neural precursor cells were then manually harvested from the periphery of neural rosettes. NPCs were further expanded with bFGF as a sole mitogen (10 ng/mg) for up to 35 passages (**Fig. 1 L**) with expression of neural precursor markers including *SOX2*, type VI intermediate filament protein (*NESTIN*), aniridia type II protein (*PAX6*) and *SRY*-box 1 (*SOX1*) (**Fig. 1 M-P**). Comparable neural precursor morphology in previously frozen and re-plated NPCs (passage 24) was also seen (**fig. S 2, A and B**). Karyotype

analysis using Giemsa banding (G-banding) demonstrated a stable karyotype in proliferating NPCs at passage 15 and 30 (**fig. S2, C and D**). Quantitative flow cytometry analysis showed $91\pm 14\%$ of SOX1⁺ cells, $51.7\pm 12\%$ of PAX6⁺, $90.8\pm 9\%$ of SOX2⁺ and $72.3\pm 17\%$ of NESTIN⁺ cells, respectively (**fig. S2 E-J**).

To characterize the multi-lineage potential of our iPSC-derived NPCs, we subcultured NPCs on an established human fetal astrocyte monolayer and then induced by withdrawal of bFGF and addition of cyclic adenosine monophosphate (cAMP), brain-derived neurotrophic factor (BDNF) and glial cell-derived neurotrophic factor (GDNF). The cultured NPCs were designed to express Enhanced Green Fluorescent Protein (EGFP) under the synapsin (SYN) promoter, and immunofluorescence staining of 8 weeks-induced NPCs showed multipolar EGFP⁺ neurons expressing doublecortin (DCX) and Fox-3 (NeuN) (**Fig. 1, R and S**). A subpopulation of DCX⁺ neurons showed gamma-aminobutyric acid (GABA) immunoreactivity (**Fig. 1T**). TUJ1 immunoreactivity was also seen (**Fig. 1U**). To assess the functionality of induced neurons in vitro, we measured spontaneous oscillation in cytosolic calcium (Ca²⁺) after loading the induced neurons with the Ca²⁺ indicator dye Fluo-4 AM. A consistent cyclical-type of calcium oscillation lasting between 4.0-17.6 seconds, suggestive of neuronal depolarization, was observed in numerous neurons (**Fig. 1V**-white boxed regions). To characterize quantitatively the number of neuronal and glial cells that can be induced from iPSCs-NPCs, proliferating NPCs were treated with 1% porcine serum for 20 days. Qualitative and quantitative analysis of induced NPCs showed effective differentiation to neurons (expressing the neuronal marker TUJ1), astrocytes [expressing the astrocyte marker glial fibrillary acidic protein (GFAP)] and glial and oligodendrocytes/precursors [(expressing VIMENTIN, chondroitin sulphate proteoglycan 4 (NG2) and oligodendrocyte transcription factor (OLIG2)], (**fig. S 2K-N**).

In vivo transplanted iPSCs-NPCs generate functional neurons at 7-10 months after grafting into striata of immunodeficient rats

We next tested the functionality of porcine iPSCs- derived NPCs (SYN-EGFP-NPCs) after grafting into the striatum of adult immunodeficient rats (**Fig. 2A**). Animals (n=12) received 3 bilateral injections of SYN-EGFP-NPCs (30,000 cells/injection; 2 μ l/injection site) into the striatum. One to ten months after cell grafting, we prepared ex vivo brain slices and performed patch clamp recordings from SYN-EGFP⁺ grafted cells (**Fig. 2B; fig. S3A**). A subset (n=6) of grafted animals was perfused with cold saline and striata harvested for mRNA sequencing (to analyze porcine-specific transcripts), (n=2; two individual NPCs-grafted striata analyzed at 10

months post-grafting) or fixed with 4% paraformaldehyde (n=4; 7 months after grafting) and the grafted cells studied with immunofluorescence staining with neuron specific antibodies (NeuN, neuron-specific enolase (NSE), DCX, SYN, vesicular GABA transporter (VGAT), gephyrin, neurofilament (NF)). A relative number (% of total EGFP+ neurons) of double-immunoreactive EGFP/DCX, EGFP/NeuN and EGFP/NSE neurons was quantified using confocal microscope (**Table S 1**).

Patch clamp recording in EGFP+ neurons showed that all the examined transplanted cells (n=3) showed properties of mature neurons, such as robust trains of action potentials (average = 18 Hz) in response to 500 ms depolarizing steps of currents (**Fig. 2C**), large voltage-gated sodium/potassium currents (Nav peak average = -5745 pA) (**Fig. 2D**), low resting membrane potentials (average = -78 mV) and spontaneous excitatory synaptic activity (**Table S 2**).

Immunofluorescence staining revealed numerous SYN-EGFP+ neurons with extensive processes in the grafted striatal regions (**Fig. 2E**). Confocal microscopy showed that virtually all SYN-EGFP+ cells colocalized with NeuN (**Fig. 2E-insets; fig. S, 3 A and B**). Similarly, intense porcine-specific, neuron-specific enolase (NSE) expression (*13*) was seen in EGFP+ grafts (**Fig. 2F; fig. S 3C**). Staining with antibodies specific for SYN and/or VGAT showed a high density of SYN/EGFP+ or SYN/VGAT+ puncta on the soma/membranes of endogenous NeuN positive neurons or EGFP+ grafted neurons (**Fig. 2, G and H; fig. S 3D**). Co-staining with presynaptic inhibitory marker (VGAT) and postsynaptic glycine receptor marker (gephyrin) showed the presence of glycine receptors on grafted EGFP+ neurons in opposition to VGAT+ terminals (**Fig. 2I; insert**) suggesting the development of inhibitory glycin-ergic synaptic contacts. Staining with NF antibody showed high density NF neural processes within EGFP+ grafts (**fig. S 3E**).

Transplanted iPSCs-NPCs are non-tumorigenic and acquire genetic signature of mature porcine CNS at 7-10 months after grafting into striata of immunodeficient rat

We next performed whole-transcriptome mRNA sequencing analysis on the striatum of immunodeficient rats that had received iPSCs-NPCs grafts (**Fig.3 A-D**). Striatal tissue was harvested 10 months after iPSCs-NPCs grafting. To separate the pig mRNA sequence reads from the host rat mRNA reads, we developed a bioinformatics pipeline to sort mRNA sequence reads in a species-specific manner to either pigs or rats (**Fig.3E**). Slight variations in the genome sequence between pigs and rats allowed us to differentiate between the species with a high sensitivity (99.52% efficiency). We detected 9332 pig genes expressed in the grafted rat striatum. This represented 5.19% of the total mRNA reads from the graft tissue, with a false positive sorting

rate of 0.47% (appendix 1), (**Table S 3**). Gene expression was analyzed with t-distributed stochastic neighbor embedding (t-SNE) to determine the global gene expression patterns in the samples. Gene expression patterns from the transplanted iPSCs-NPCs correlated strongly with the expression pattern of control mature pig CNS tissue, but not with the original iPSCs-NPCs or iPS cell populations (**Fig. 3F**). Analysis of mature CNS-specific transcripts in grafted cells shows high expression of neuronal markers and only moderate to low expression of glial genes (**fig. S, 3F and G**). These data indicate that transplanted iPSCs-derived NPCs differentiate normally into neuronal and glial subtypes, and adopt gene expression patterns indicative of the environment into which they were grafted.

To identify any neuropathologically-defined signs of tumor formation, sections were also stained using H&E. Consistent with immunofluorescence staining, well incorporated grafts that fused with the host tissue were identified. No gross signs of tissue necrosis or aberrant tissue proliferation were noted (**fig. S 4A**). Staining with myelin basic protein (MBP) and OLIG2 antibody showed incomplete myelination in EGFP+ grafts which was in contrast with the surrounding host tissue (**fig. S 4 B-D**). In the same areas the presence of VIMENTIN+ cells and oligodendrocytes (OLIG2+) was also seen suggesting ongoing myelination (**fig. S 4 E-G**).

Staining with endothelial marker Recla-1 showed regularly distributed vessel profiles in EGFP+ grafts (**fig. S 5, A and B**). The expression of a subset of proto-oncogenes and tumor suppressor genes in grafted rat striata at 10 months post-grafting was very similar to that observed in normal control pig spinal cord and striatum tissue (**fig. S 5C**).

Collectively, these data show that we have generated a transplantable, non-tumorigenic population of porcine iPSCs-derived NPCs that shows a robust neuronal differentiation and is functional once grafted into the adult CNS of immunodeficient rats.

Syngeneic porcine iPSCs-NPCs grafted spinally in adult naive pigs show long-term survival in the absence of immunosuppression

We next tested if the syngeneic transplantation of porcine iPSCs-NPCs into the lumbar spinal cord of naive spinally-non-injured pigs would support cell survival in the absence of immunosuppression. Three SLA fully-matched minipigs received 20 bilateral syngeneic grafts of iPSCs-NPCs (SYN-EGFP+) targeted into the central gray matter of the L2-L5 spinal cord segments (50,000 live cells/ μ l, 10 μ l/injection). Three months after grafting the animals were sacrificed and the spinal cord harvested for subsequent analysis.

Immunofluorescence analysis of horizontal spinal cord sections throughout the grafted region showed the presence of long bilateral EGFP+ grafts extending for more than 2 cm (**Fig. 4A**, **fig. S 6A**). No tumor formation or aberrant tissue mass was seen in any animal. High density NF-positive and GFAP-positive networks were identified in EGFP+ grafts (**Fig. 4, B and C; fig. S 6, B and C**). Staining with neuron-specific markers including DCX, NeuN and NSE showed neurons that occupied the entire EGFP+ grafts (**Fig. 4 D-F; fig. S 6 D-F**). Analysis of axonal projections into regions caudal and cranial from the border of the EGFP+ graft showed the projection of EGFP+ axons for distances longer than 2-3 cm. These axons showed co-expression of NF (**Fig. 4 G-I**). A quantitative analysis (% of total EGFP+ neurons) of double-immunoreactive EGFP/DCX, EGFP/NeuN and EGFP/NSE neurons is presented in **Table S 1**.

Staining with SYN antibody revealed a high density of SYN+ puncta throughout the EGFP+ graft (**fig. S 6 G**). The majority of EGFP/SYN+ puncta displayed colocalization with VGAT and was opposed to a postsynaptic gephyrin+ puncta found on EGFP+ grafted neurons or EGFP-negative host neurons (**Fig. 4 J and K; fig. S 6 G**). These data demonstrate the development of putative inhibitory synaptic contacts.

Syngeneic pigs receiving spinal iPSCs-NSCs grafts show no humoral immunity against grafted cells at 3 months after cell transplantation

To test for the presence of circulating anti-iPSCs-NPCs antibodies in syngeneic pigs grafted spinally with iPSCs-NPCs, a combined in vivo and ex vivo immunostaining assay was developed. First, a homogenate mixture composed of proliferating or induced iPSCs-NPCs (in Freund's adjuvant; non-EGFP-tagged cells) was injected subcutaneously to immunize an allogeneic pig (**Fig. 5 A**). In parallel, the same NPCs population (but expressing EGFP under SYN promoter) was injected into the striata or lumbar spinal cord in immunodeficient rats. Six months after grafting, rat brain and spinal cord sections containing iPSCs-NPCs-EGFP were harvested and stained using the sera taken from immunized pig (positive control), naive non-immunized allogeneic pig (negative control) and syngeneic pigs that had previously received spinal iPSCs-NPCs-EGFP grafts.

Staining of rat striatal and spinal cord sections (harvested at 6 months post-grafting) containing iPSCs-NPCs-EGFP+ grafts with pig sera from immunized pigs showed cellular staining in grafted EGFP+ neurons (positive control, **Fig. 5 B**). No staining was observed with sera taken from non-immunized pigs (negative control) or from a syngeneic pig grafted spinally with iPSCs-NPCs-EGFP (**Fig. 5, C and D**). These data demonstrate that no humoral immune reaction developed in syngeneic pig for a minimum of 3 months after cell grafting.

Short-term immunosuppression (4 weeks) induces immune tolerance to allogeneic iPSCs-NPCs grafted spinally in adult pigs with previous chronic spinal traumatic injury

We next tested if porcine iPSCs-NPCs (the same cell line as used for syngeneic spinal grafting) could survive and differentiate after transplantation into the lumbar spinal cord of allogeneic pigs in the context of both spinal cord injury and transient (1 month) immunosuppression. Allogeneic minipigs (n=3) that had undergone a spinal cord injury in the L3 segment received 20 bilateral grafts of iPSCs-NPCs-EGFP (under ubiquitin (UBI) promoter; 50,000 live cells/ μ l, 10 μ l/injection) 2.5 months after spinal trauma. After cell grafting animals were immunosuppressed for 4 weeks with Prograf (0.025 mg/kg/day; iv). After an additional 2.5 months without immunosuppression, the presence of grafted cells was analyzed in spinal cord sections using immunofluorescence (**Fig.6A**). The relative number (% of total EGFP+ neurons, astrocytes and oligodendrocytes) of double-immunoreactive EGFP/DCX, EGFP/NeuN, EGFP/NSE neurons and EGFP/GFAP and EGFP/OLIG2 glial cells was quantified using 4 sections/animal containing a clearly identifiable EGFP+ graft. The degree of SLA mismatch between the iPSCs-NPCs donor and graft recipients was analyzed in skin fibroblast DNA extracts using PCR-based SLA genotyping assays (14, 15).

The injured spinal cord regions were found to be extensively populated by grafted NPCS-EGFP+ cells in all 3 animals. The length of individual fused grafts ranged between 2-3 cm (**Fig. 6 B, C; fig. S 7 A**). Staining with NeuN antibody showed NeuN+ neurons throughout the EGFP+ grafts (**Fig. 6 B, D-F**). A high density of SYN expression in EGFP+ grafts was also observed and was similar to that seen in the surrounding host tissue (**Fig. 6 B; top right insert**). Co-staining with NeuN and NF antibody showed a high density NF+ neurites in NeuN populated grafts (**Fig. 6 G**). Staining with DCX and NSE antibody showed numerous DCX/NSE-expressing EGFP+ neurons at different stages of neuronal maturation (**Fig. 6 H; fig. 7 S B-E**). Triple staining with SYN, EGFP and VGAT antibodies confirmed a high density of SYN/VGAT terminals associated with EGFP puncta (**Fig. 6 I; fig. S 7F**). EGFP/SYN/VGAT+ puncta were opposed to a postsynaptic gephyrin+ puncta seen on EGFP+ grafted neurons or EGFP-negative host neurons (**Fig. 6J; fig. S 7G**). Staining with postsynaptic excitatory marker Homer 1 (postsynaptic protein associated with group 1 metabotropic glutamate receptor) showed a clear punctate-like staining on neuronal soma and axons of EGFP+ grafted neurons (**Fig. 6 K; fig. S 7 H**).

Staining with GFAP and OLIG2 antibodies revealed graft-derived astrocytes and oligodendrocytes (**Fig. 6 L-N; fig. S 7I**). Co-staining with choline acetyltransferase (CHAT) antibody showed the occasional presence of CHAT+ neurons (**fig. S 7J**). Detailed regional

analysis of NeuN expression in UBI-EGFP-grafted regions showed homogenous distribution of NeuN⁺ neurons through the whole engrafted region (**fig. S 8 A-D**). A quantitative analysis (% of total EGFP⁺ neurons) of double-immunoreactive EGFP/DCX, EGFP/NeuN, EGFP/NSE, EGFP/GFAP and EGFP/OLIG2 neurons and glial cells is presented in **Table S 1**.

The H&E staining showed well-incorporated individual grafts with morphology consistent with mature neural tissue (**fig. S 9A**). In comparison with the host surrounding tissue, incomplete myelination was observed, as evidenced by a low density of MBP immunoreactivity within EGFP⁺ grafts (**fig. S 9, B and C**). Numerous triple-stained EGFP/VIMENTIN/Ki67⁺ cells were found within EGFP⁺ grafts (**fig. S 9D-insets, E**). These data suggest ongoing myelination and proliferation of glial precursors. To study the dynamics of cell proliferation (Ki67⁺ cells) in developing porcine spinal cord, we next stained spinal cord sections prepared from 70-days-old porcine fetus (gestational period in pig is around 115 days), newborn piglet and adult naive pig (18 months old). In the 70-day-old fetus a high density of Ki67⁺ cells in both white and gray matter regions was seen. The number of Ki67⁺ cells decreased in newborn piglets but was still present in the adult pig (**fig. S 9 F-I**). These data are consistent with a previous report in mice which demonstrated an ongoing proliferation of glial precursors in the intact adult spinal cord (16).

Transiently-immunosuppressed (4 weeks) allogeneic, spinally-injured pigs show no humoral or cellular immunity against grafted iPSCs-NPCs at 2.5 months after cell transplantation

Next, we tested the presence of circulating antibodies against iPSCs-NPCs by staining mature (6 months post-grafting) iPSCs-NPCs grafts in the rat striata with sera harvested from allogeneic iPSCs-NPCs-grafted pigs. In contrast to the strong staining observed with sera from anti-iPSCs-NPCs-immunized pig, no staining was detected with sera from allogeneic graft recipients (**Fig. 6, O and P**). As shown in **Table S 4, A and B**, the SLA genotypes of the iPSCs-NPCs donor and the allogeneic graft recipients were well mismatched at both the antigen (allele-group) and allele level across the class I (*SLA-1, SLA-2, SLA-3*) and class II (*DRB1, DQA, DQB1*) loci tested (17-23).

To further probe for the presence of an immune response in cell-grafted spinal cord regions, spinal sections were stained with porcine-specific anti- major histocompatibility complex II (MHC-II), CD45 (leukocyte common antigen), CD8 (co-receptor for the T cell receptor) and ionized calcium-binding adapter molecule 1 (Iba1; microglial marker) antibodies. Sections were taken from: **i)** spinal cord of syngeneic pigs 3 months after iPSCs-NPCs grafting without

immunosuppression, **ii**) spinal cord of injured, continuously-immunosuppressed allogeneic pigs 4 weeks after iPSCs-NPCs grafting, and **iii**) spinal cord of injured, transiently-immunosuppressed allogeneic pigs 3.5 months after iPSCs-NPCs grafting. In syngeneic pigs the staining with anti-MHC-II antibody showed that the immunoreactivity was restricted around the needle injection tracts (**Fig. 7A**). In allogeneic spinally-injured animals with continuous or transient immunosuppression a more diffuse staining pattern was seen and MHC-II+ cells were observed throughout the EGFP+ graft as well as in surrounding injured host tissue (**Fig. 7, B and C**). Staining with Iba1 antibody exhibited a very similar staining pattern as was seen for MHC-II staining (**Fig. 7 D-F**). Staining with CD45 and CD8 antibody showed accumulation of both cell types around the cell injection tract in syngeneic pigs and more diffuse presence of CD45/CD8-positive cells in allogeneic spinally-injured pigs with continuous or transient immunosuppression (**Fig. 7 G-I**). Analysis of double MHC-II and Iba1-stained sections showed that virtually all MHC-II+ cells expressed Iba1 (**Fig. 7J**). Quantitative comparative analysis of CD45 and CD8 positive cells between allogeneic spinally-injured continuously-immunosuppressed animals (1-month post-grafting survival) and animals with transient immunosuppression 3 months after grafting showed a significant decrease in the number of both CD45+ and CD8+ cells 3 months after cell grafting in transiently immunosuppressed animals (**Fig. 7, K and L**).

These data demonstrate that spinal grafting of iPSCs-NPCs in syngeneic non-immunosuppressed or allogeneic transiently-immunosuppressed animals leads to a robust graft survival with minimal immune response at the site of cell grafting.

Analysis of neurological function in allogeneic NPC-grafted animals 3.5 months after grafting was performed using a previously developed porcine neurological scale designed to quantify the loss of motor function after spinal cord traumatic injury in adult pigs (24). Grade “0” corresponds with complete paraplegia with no detectable movement in the hind limbs and grade “14” corresponds with normal ambulatory function. NPCs-grafted animals showed 2-3 degrees improvement (from grade 6 to grade 8 or 9) compared to pre-transplantation baseline. This corresponds to better movement in all three joints of lower extremities but with no ability to support weight or walk.

Reprogramming factors and immunogenic genes are not expressed in vivo in grafted iPSCs-NPCs

We next studied the residual protein expression of reprogramming factors (OCT4, KLF4 and SOX2) and Sendai virus-associated protein (SeV) in grafted cells at 3 and 7 months post-grafting by using sections taken from grafted rat striata and allogeneic pig spinal cord. Sections

were also stained with Ki67 antibody. Staining with OCT4 and KLF4 antibody showed no residual staining in grafted cells (**fig. S 10A-H**). Staining with SOX2 antibody showed regularly distributed SOX2+ cells within EGFP+ grafts in both rat striata and allogeneic pig spinal cord (**fig. S 10 I-L**). In allogeneic pig spinal cord a specific SOX2 expression was also seen in endogenous ependymal cells of central canal (**fig. S 10L**; white dotted line). Staining with Ki67 antibody showed regularly distributed double EGFP/Ki67-stained cells in both rat striata and allogeneic pig spinal cord grafts. (**fig. S 10 M-P**). Staining with anti-SeV antibody revealed only occasional presence of Sendai virus-associated protein in grafted EGFP+ cells (**fig. S 11 A-D**). The mRNA sequencing analysis showed no apparent differences in several immunogenic genes including Hormad 1 and Cyp39A1 (**fig. S 11E**).

DISCUSSION

Using non-integrating Sendai virus (encoding *OCT4*, *SOX2*, *KLF4* and *c-MYC*) we demonstrated the successful reprogramming of porcine skin fibroblasts harvested from adult fully SLA-matched pigs to iPSCs. After iPSCs induction, we isolated the NPCs by manual selection and expanded for more than 20 passages while maintaining a stable karyotype and expressing markers typical of NPCs (such as *SOX1*, *SOX2*, *NESTIN* and *PAX6*). Once grafted into the striata of immunodeficient rats or the spinal cord of syngeneic naive-non-injured pigs in the absence of immunosuppression, NPCs differentiated into functional neurons and glial cells (astrocytes, oligodendrocytes). Consistent with an advanced stage of grafted NPCs maturation, the mRNA sequencing analysis of porcine-specific transcripts in rat striata at 10 months post-grafting showed a pattern of expression similar to control mature pig CNS tissue. Moreover, long-term survival of iPSCs-NPCs-derived cells was observed after grafting into spinal cord-injured allogeneic pigs that had received only transient immunosuppression.

Previous study have reported immunogenicity from syngeneic mouse iPSCs upon transplantation that may be related to an ongoing overexpression of pluripotent genes (25). In addition, several other factors such as expression of virus-related proteins generated by episomal vectors used for reprogramming and the MHC expression in specific iPSC-cell derivatives may contribute to overall immunogenicity of transplanted cells (25). We have addressed those issues and have demonstrated that i) there is no expression of pluripotent genes at 3-7 months post-transplantation, and ii) only occasional Sendai virus-associated protein was present in grafted iPSCs-NPCs. These data suggest that, although a residual Sendai viral protein is present at the

moment of grafting, it is not sufficient to trigger hyper-acute or late T-cell mediated rejection. We have also demonstrated a lack of humoral or cellular response in syngeneic and allogeneic pigs receiving iPSCs-NPCs grafts. These data further demonstrate that even a mature iPSCs-NPCs graft does not express antigens which would be sufficient to initiate an immune response at prolonged periods after grafting.

In addition, there are several other variables which we believe need to be considered while generating iPSCs-derived transplantable cell lines for experimental or clinical application. It has been demonstrated that several genes are expressed at abnormally high levels in mouse iPSCs. A subset of upregulated genes with known immunogenic properties, including *Hormad1*, *Zg16* and *Cyp3a11*, has been found to be directly linked to the T-cell mediated rejection of teratomas that formed after grafting of mouse iPS cell lines into syngeneic recipients (25). All the iPSCs used in this previous study (13) came from fetal fibroblasts, an unlikely source for future therapies in humans, and the gene expression changes may be related to epigenetic memory of this specific developmental time. The use of adult fibroblast in our current experiments may contribute to the lack of immunogenic gene upregulation.

Altered gene expression can be also due to the transcriptional memory observed in iPSCs (26, 27) or caused by somatic alterations in protein-coding regions accumulated in these cells (28). Whether there is increased activity of potentially immunogenic proteins in long-term expanded iPSCs-derived cell lines is not defined at present. Thus a periodic analysis of such changes needs to be performed to assure consistency of the genetic profile across specific lots of transplantable cells.

We have previously demonstrated that culturing human ES cells in the presence of animal components, such as mouse feeder cells or bovine albumin, leads to the incorporation of animal molecules in the membranes of human cells (29). These molecules, such as *N*-glycolylneuraminic acid (Neu5Gc), contaminated human ES cells and initiated an antibody-mediated complement deposition when the cells were exposed to human sera. Accordingly, in our current study, to avoid the contamination of generated iPSCs by non-porcine animal component(s) we have used porcine fetal skin-derived fibroblasts as a feeder layer and no serum derived from other animal species was used. Thus, the derived iPSCs-NPCs had no non-porcine elements in their membranes that can elicit an immune reaction in the syngeneic or allogeneic graft recipients.

Previous studies reported the transplantation of iPSCs-derived dopaminergic precursors using intrastriatal autologous or allogeneic grafting in non-human primates without immunosuppression (30, 31). Minimal or no immune response was seen in autologous grafts while

a progressive acquired immune response was seen in allogeneic graft recipients at 3.5-4 months after cell grafting. We show that the transient immunosuppression protocol used in our current study is effective in inducing a long-term graft tolerance in allogeneic spinally-injured and SLA-mismatched recipients. These results are similar to our previously reported data which demonstrate tolerance across a two-haplotype, fully MHC-mismatched barrier in miniature swine renal allografts after transient (12 days) high-dose treatment with tacrolimus (32). More recently, a functional engraftment of allogeneic iPSCs-derived cardiomyocytes after a direct intra-myocardial injection in the cynomolgus monkey model of myocardial infarction was reported. In this experiment, continuous immunosuppression with tacrolimus was used (33). Other groups have reported on functional benefit after spinal grafting of human iPSCs-NPCs in mouse and marmoset spinal injury models (34, 35) and also demonstrated low immunogenicity of mouse iPSCs-derived NPCs (36, 37).

Since the spinal cord and brain represent sites of immune privilege, it has long been speculated that only transient immune suppression is sufficient to ensure long-term engraftment of human fetal tissue-derived or iPSCs-derived NPCs in human allogeneic graft recipients. Thus, our findings demonstrate in a large animal model of spinal cord traumatic injury that in fact a transient 4-week immunosuppression is effective in inducing immune tolerance against allogeneic iPSCs-NPCs grafts. One limitation of our current study is that a relatively short post-grafting period of survival was used in pig component of the study. Accordingly, a prolonged postgrafting survival likely exceeding 1 year will be needed to confirm a permanent iPSCs-NPCs engraftment once cells are grafted into syngeneic or allogeneic transiently-immunosuppressed recipients.

Our pre-clinical large animal model system will allow us to establish prospective assays to predict graft rejection in the context of autologous, syngeneic or allogeneic grafting of iPSCs-derived neural precursors in naive or previously-injured spinal cord. Similar to the studies from Zhao *et al.* (25), we expect that a profiling of gene regulation, membrane-bound and soluble-releasable proteins that have immunogenic properties, and recipient T-cell activation assays, will be important in determining the immunogenicity of prospective iPSCs-derived lineage-committed cell lines to be used for in vivo grafting. In this manner, the degree of immune suppression could be personalized to the quantity of recipient T cell reactivity to graft antigens, thereby ensuring that appropriate immune suppression is used.

MATERIAL and METHODS

Study design

This study was designed to characterize the survival of porcine iPSCs-NPCs after spinal grafting in adult naive syngeneic (non-immunosuppressed) or chronic spinally-injured allogeneic (transiently immunosuppressed) pigs. To generate pluripotent cells, we used sendai virus encoding 4 reprogramming factors to reprogram adult pig fibroblasts (harvested from inbred SLA-matched pigs) in vitro. Pluripotent nature of established iPSCs colonies was determined by in vitro induction into all 3 germ layers (ectoderm, mesoderm, endoderm) and by the formation of in vivo teratoma. NPCs were then induced from pluripotent colonies using NSC-induction protocol and established NPCs characterized in vitro and in vivo by: i) expression of NPCs markers (flow cytometry or indirect immunofluorescence, ii) ability of neurons to spontaneously depolarize after long-term in vitro induction (Ca^{2+} oscillation), and iii) ability of iPSC-derived neurons to generate action potential in ex-vivo striatal slices. To study a multipotent potential of established iPSCs-NPCs cells (SYN-EGFP) grafted into rat striata, we used immunofluorescence staining using neuronal and glial markers and mRNA sequencing using bioinformatics protocol which separates the pig mRNA sequence reads from the host rat mRNA reads. Neurotransmitter phenotype of grafted iPSCs-NPCs-derived neurons was studied in EGFP⁺ grafts in rat striata and pig spinal cord by immunofluorescence staining with pre- and post-synaptic markers specific for inhibitory or excitatory neuronal phenotype.

For quantitative analysis of immune response markers (CD45 and CD8) spinal cord sections taken from iPSCs-NPC-grafted: i) syngeneic pigs, ii) allogeneic pigs at the end of 4 weeks immunosuppression, and iii) allogeneic pigs at 2.5 months after immunosuppression was terminated, were used. The presence of positively-stained CD45 and CD8 cells was analyzed separately in the EGFP⁺ grafts and in surrounding host tissue.

Full details on the methods of in vitro iPSCs and iPSCs-NPCs generation/characterization and in vivo iPSCs-NPCs grafting and post-mortem analysis can be found in the Supplementary Materials.

Statistical analysis

For statistical analysis the number of positively-stained (CD45⁺ and CD8⁺) cells in allogeneic animals (pigs) with continuous and transient immunosuppression was compared using unpaired, two-tailed Student's T-test for single comparisons. Data were considered significantly different if $P < 0.05$. GraphPad Prism software was used to run Student's tests.

Supplementary Materials

Supplementary Methods

fig.S1. Porcine fibroblasts-derived iPSC generate ectoderm, mesoderm and endoderm cell derivatives in vitro and in vivo.

fig.S2. Previously frozen, in vitro expanded porcine iPSCs-derived NPCs show stable karyotype and generate neural derivatives (neurons, astrocytes and oligodendrocytes) after in vitro induction.

fig.S3. Long-term grafted (7-10 months) porcine iPSCs-NPCs in rat striata show maturation protein- and mRNA signature which is consistent with mature porcine CNS tissue.

fig.S4. Porcine iPSCs-NPCs grafted into rat striata show no tumor formation and incomplete myelination at 7 months postgrafting.

fig.S5. Porcine iPSCs-NPCs –EGFP+ grafts in rat striata show normal vascularization and no changes in tumor suppressors or proto-oncogenes at 7-10 months post-grafting.

fig.S6. iPSCs-NPCs grafted into syngeneic pig spinal cord in the absence of immunosuppression show long-term survival and neuronal and glial differentiation at 3 months after transplantation.

fig.S7. iPSCs-NPCs grafted spinally in allogeneic, transiently-immunosuppressed (1 month immunosuppression) pigs with previous spinal traumatic injury show neuronal and glial differentiation at 3.5 months after grafting.

fig.S8. Spinally-grafted iPSCs-NPCs in allogeneic, spinally-injured pig with transient immunosuppression (1 month) show extensive neuronal (NeuN) differentiation at 3.5 months after grafting.

fig.S9. iPSCs-NPCs grafted spinally in allogeneic pig with previous spinal injury don't form tumors and show incomplete myelination at 3.5 months postgrafting.

fig.S10. Reprogramming factors (*OCT4*, *KLF4*) are silenced in mature iPSCs-NPCs grafts in rat striata or spinal cord in allogeneic pig with previous spinal traumatic injury.

fig.S11. Long-term grafted iPSCs-NPCs in rat striata or spinal cord of allogeneic pig show only occasional presence of Sendai virus-associated protein in grafted cells and show no change in expression of immunogenic genes.

Table S 1. Quantitative analysis of neuronal and glial differentiation in EGFP grafts.

Table S 2. Electrophysiological properties of three transplanted iPSC neurons into the striatum of a rat at 8 months post-grafting.

Table S 3. mRNA sequencing species sorting quantification.

Table S 4A. SLA haplotypes of donor iPSCs-NPCs and allogeneic graft recipients.

Table S 4B. Expected high-resolution (Hp) SLA typing and haplotype.

Table S 5. Antibodies used for Flow cytometry, and immunofluorescence staining.

References

1. K. Takahashi, S. Yamanaka, Induction of pluripotent stem cells from mouse embryonic and adult fibroblast cultures by defined factors. *Cell* **126**, 663-676 (2006).
2. K. Takahashi, K. Tanabe, M. Ohnuki, M. Narita, T. Ichisaka, K. Tomoda, S. Yamanaka, Induction of pluripotent stem cells from adult human fibroblasts by defined factors. *Cell* **131**, 861-872 (2007).
3. M. C. Marchetto, K. J. Brennand, L. F. Boyer, F. H. Gage, Induced pluripotent stem cells (iPSCs) and neurological disease modeling: progress and promises. *Hum Mol Genet* **20**, R109-115 (2011).
4. A. R. Muotri, Modeling epilepsy with pluripotent human cells. *Epilepsy Behav* **14 Suppl 1**, 81-85 (2009).
5. R. M. Roberts, B. P. Telugu, T. Ezashi, Induced pluripotent stem cells from swine (*Sus scrofa*): why they may prove to be important. *Cell Cycle* **8**, 3078-3081 (2009).
6. B. P. Telugu, T. Ezashi, R. M. Roberts, Porcine induced pluripotent stem cells analogous to naive and primed embryonic stem cells of the mouse. *Int J Dev Biol* **54**, 1703-1711 (2010).
7. B. P. Telugu, T. Ezashi, R. M. Roberts, The promise of stem cell research in pigs and other ungulate species. *Stem Cell Rev* **6**, 31-41 (2010).
8. M. A. Esteban, J. Xu, J. Yang, M. Peng, D. Qin, W. Li, Z. Jiang, J. Chen, K. Deng, M. Zhong, J. Cai, L. Lai, D. Pei, Generation of induced pluripotent stem cell lines from Tibetan miniature pig. *J Biol Chem* **284**, 17634-17640 (2009).
9. M. A. Esteban, M. Peng, Z. Deli, J. Cai, J. Yang, J. Xu, L. Lai, D. Pei, Porcine induced pluripotent stem cells may bridge the gap between mouse and human iPS. *IUBMB Life* **62**, 277-282 (2010).
10. T. Ezashi, B. P. Telugu, A. P. Alexenko, S. Sachdev, S. Sinha, R. M. Roberts, Derivation of induced pluripotent stem cells from pig somatic cells. *Proc Natl Acad Sci U S A* **106**, 10993-10998 (2009).
11. Z. Wu, J. Chen, J. Ren, L. Bao, J. Liao, C. Cui, L. Rao, H. Li, Y. Gu, H. Dai, H. Zhu, X. Teng, L. Cheng, L. Xiao, Generation of pig induced pluripotent stem cells with a drug-inducible system. *J Mol Cell Biol* **1**, 46-54 (2009).
12. N. Fusaki, H. Ban, A. Nishiyama, K. Saeki, M. Hasegawa, Efficient induction of transgene-free human pluripotent stem cells using a vector based on Sendai virus, an RNA virus that does not integrate into the host genome. *Proc Jpn Acad Ser B Phys Biol Sci* **85**, 348-362 (2009).
13. D. Usvald, P. Vodicka, J. Hlucilova, R. Prochazka, J. Motlik, J. Strnadel, K. Kucharova, K. Johe, S. Marsala, M. Scadeng, O. Kakinohana, R. Navarro, M. Santa, M. P. Hefferan, T. L. Yaksh, M. Marsala, Analysis of dosing regimen and reproducibility of intraspinal grafting of human spinal stem cells in immunosuppressed minipigs. *Cell Transplant* **19**, 1103-1122 (2010).
14. C. S. Ho, J. K. Lunney, M. H. Franzo-Romain, G. W. Martens, Y. J. Lee, J. H. Lee, M. Wysocki, R. R. Rowland, D. M. Smith, Molecular characterization of swine leucocyte antigen class I genes in outbred pig populations. *Anim Genet* **40**, 468-478 (2009).
15. C. S. Ho, J. K. Lunney, J. H. Lee, M. H. Franzo-Romain, G. W. Martens, R. R. Rowland, D. M. Smith, Molecular characterization of swine leucocyte antigen class II genes in outbred pig populations. *Anim Genet* **41**, 428-432 (2010).
16. F. Barnabe-Heider, C. Goritz, H. Sabelstrom, H. Takebayashi, F. W. Pfriederger, K. Meletis, J. Frisen, Origin of new glial cells in intact and injured adult spinal cord. *Cell Stem Cell* **7**, 470-482 (2010).
17. C. S. Ho, M. H. Franzo-Romain, Y. J. Lee, J. H. Lee, D. M. Smith, Sequence-based characterization of swine leucocyte antigen alleles in commercially available porcine cell lines. *Int J Immunogenet* **36**, 231-234 (2009).
18. C. S. Ho, E. S. Rochelle, G. W. Martens, L. B. Schook, D. M. Smith, Characterization of swine leucocyte antigen polymorphism by sequence-based and PCR-SSP methods in Meishan pigs. *Immunogenetics* **58**, 873-882 (2006).

19. D. M. Smith, G. W. Martens, C. S. Ho, J. M. Asbury, DNA sequence based typing of swine leukocyte antigens in Yucatan miniature pigs. *Xenotransplantation* **12**, 481-488 (2005).
20. C. S. Ho, G. W. Martens, M. S. Amoss, Jr., L. Gomez-Raya, C. W. Beattie, D. M. Smith, Swine leukocyte antigen (SLA) diversity in Sinclair and Hanford swine. *Dev Comp Immunol* **34**, 250-257 (2010).
21. S. E. Essler, W. Ertl, J. Deutsch, B. C. Ruetgen, S. Groiss, M. Stadler, B. Wysoudil, W. Gerner, C. S. Ho, A. Saalmueller, Molecular characterization of swine leukocyte antigen gene diversity in purebred Pietrain pigs. *Anim Genet* **44**, 202-205 (2013).
22. Y. J. Lee, K. H. Cho, M. J. Kim, D. M. Smith, C. S. Ho, K. C. Jung, D. I. Jin, C. S. Park, J. T. Jeon, J. H. Lee, Sequence-based characterization of the eight SLA loci in Korean native pigs. *Int J Immunogenet* **35**, 333-334 (2008).
23. H. O. Cho, C. S. Ho, Y. J. Lee, I. C. Cho, S. S. Lee, M. S. Ko, C. Park, D. M. Smith, J. T. Jeon, J. H. Lee, Establishment of a resource population of SLA haplotype-defined Korean native pigs. *Mol Cells* **29**, 493-499 (2010).
24. R. Navarro, S. Juhas, S. Keshavarzi, J. Juhasova, J. Motlik, K. Johe, S. Marsala, M. Scadeng, P. Lazar, Z. Tomori, G. Schulteis, M. Beattie, J. D. Ciacci, M. Marsala, Chronic spinal compression model in minipigs: a systematic behavioral, qualitative, and quantitative neuropathological study. *J Neurotrauma* **29**, 499-513 (2012).
25. T. Zhao, Z. N. Zhang, Z. Rong, Y. Xu, Immunogenicity of induced pluripotent stem cells. *Nature* **474**, 212-215 (2011).
26. M. C. Marchetto, G. W. Yeo, O. Kainohana, M. Marsala, F. H. Gage, A. R. Muotri, Transcriptional signature and memory retention of human-induced pluripotent stem cells. *PLoS One* **4**, e7076 (2009).
27. M. H. Chin, M. J. Mason, W. Xie, S. Volinia, M. Singer, C. Peterson, G. Ambartsumyan, O. Aimiwu, L. Richter, J. Zhang, I. Khvorostov, V. Ott, M. Grunstein, N. Lavon, N. Benvenisty, C. M. Croce, A. T. Clark, T. Baxter, A. D. Pyle, M. A. Teitell, M. Pelegrini, K. Plath, W. E. Lowry, Induced pluripotent stem cells and embryonic stem cells are distinguished by gene expression signatures. *Cell Stem Cell* **5**, 111-123 (2009).
28. A. Gore, Z. Li, H. L. Fung, J. E. Young, S. Agarwal, J. Antosiewicz-Bourget, I. Canto, A. Giorgetti, M. A. Israel, E. Kiskinis, J. H. Lee, Y. H. Loh, P. D. Manos, N. Montserrat, A. D. Panopoulos, S. Ruiz, M. L. Wilbert, J. Yu, E. F. Kirkness, J. C. Izpisua Belmonte, D. J. Rossi, J. A. Thomson, K. Eggan, G. Q. Daley, L. S. Goldstein, K. Zhang, Somatic coding mutations in human induced pluripotent stem cells. *Nature* **471**, 63-67 (2011).
29. M. J. Martin, A. Muotri, F. Gage, A. Varki, Human embryonic stem cells express an immunogenic nonhuman sialic acid. *Nat Med* **11**, 228-232 (2005).
30. A. Morizane, D. Doi, T. Kikuchi, K. Okita, A. Hotta, T. Kawasaki, T. Hayashi, H. Onoe, T. Shiina, S. Yamanaka, J. Takahashi, Direct comparison of autologous and allogeneic transplantation of iPSC-derived neural cells in the brain of a non-human primate. *Stem Cell Reports* **1**, 283-292 (2013).
31. A. Morizane, T. Kikuchi, T. Hayashi, H. Mizuma, S. Takara, H. Doi, A. Mawatari, M. F. Glasser, T. Shiina, H. Ishigaki, Y. Itoh, K. Okita, E. Yamasaki, D. Doi, H. Onoe, K. Ogasawara, S. Yamanaka, J. Takahashi, MHC matching improves engraftment of iPSC-derived neurons in non-human primates. *Nat Commun* **8**, 385 (2017).
32. R. Utsugi, R. N. Barth, H. Kitamura, J. Ambroz, D. H. Sachs, K. Yamada, Tolerance across a two-haplotype, fully MHC-mismatched barrier induced in miniature swine renal allografts treated with a 12-day course of tacrolimus. *Transplant Proc* **33**, 101 (2001).
33. Y. Shiba, T. Gomibuchi, T. Seto, Y. Wada, H. Ichimura, Y. Tanaka, T. Ogasawara, K. Okada, N. Shiba, K. Sakamoto, D. Ido, T. Shiina, M. Ohkura, J. Nakai, N. Uno, Y. Kazuki, M. Oshimura, I. Minami, U. Ikeda, Allogeneic transplantation of iPSC cell-derived cardiomyocytes regenerates primate hearts. *Nature*, (2016).

34. S. Nori, Y. Okada, A. Yasuda, O. Tsuji, Y. Takahashi, Y. Kobayashi, K. Fujiyoshi, M. Koike, Y. Uchiyama, E. Ikeda, Y. Toyama, S. Yamanaka, M. Nakamura, H. Okano, Grafted human-induced pluripotent stem-cell-derived neurospheres promote motor functional recovery after spinal cord injury in mice. *Proc Natl Acad Sci U S A* **108**, 16825-16830 (2011).
35. Y. Kobayashi, Y. Okada, G. Itakura, H. Iwai, S. Nishimura, A. Yasuda, S. Nori, K. Hikishima, T. Konomi, K. Fujiyoshi, O. Tsuji, Y. Toyama, S. Yamanaka, M. Nakamura, H. Okano, Pre-evaluated safe human iPSC-derived neural stem cells promote functional recovery after spinal cord injury in common marmoset without tumorigenicity. *PLoS One* **7**, e52787 (2012).
36. G. Itakura, M. Ozaki, N. Nagoshi, S. Kawabata, Y. Nishiyama, K. Sugai, T. Iida, R. Kashiwagi, T. Ookubo, K. Yastake, K. Matsubayashi, J. Kohyama, A. Iwanami, M. Matsumoto, M. Nakamura, H. Okano, Low immunogenicity of mouse induced pluripotent stem cell-derived neural stem/progenitor cells. *Sci Rep* **7**, 12996 (2017).
37. H. Okano, M. Nakamura, K. Yoshida, Y. Okada, O. Tsuji, S. Nori, E. Ikeda, S. Yamanaka, K. Miura, Steps toward safe cell therapy using induced pluripotent stem cells. *Circ Res* **112**, 523-533 (2013).

Acknowledgments

We thank the following people for their technical assistance during rat and minipig surgeries and post surgery animal care: Camila Santucci, Sandee Nguyen, Dr. Alice Smith, DVM, Dr. Kent Osborn, DVM, Dr. Keith Jenne, DVM, Dr. Jennifer Fujimoto, DVM, Dr. Sarah Leonhard, DVM, Marilyn Hardee, Jessica Maryo, Miyoko Yamamoto, Crystal Bennett, Lori Teare, Megan Bokar, Jason Ring, Alex Guardado, Daniel Dunne and Amber Millen for her help with manuscript preparation. We also thank Nissi Varki, MD for her neuropathological expertise and help in evaluating H&E-stained slides.

Funding

JS, MPH, DSG, JAC, OP, REN and OK were partially supported by the CIRM Comprehensive Grant and Immunology-Transplantation grant (RC1-00131-1; RM1-01720; Martin Marsala, Jack Bui). Sanford Consortium for Regenerative Medicine (SANPORC; MM), JS was partially supported by Czech Academy of Sciences (IRP IAPG No. AV0Z50450515), UCSD Neuroscience Microscopy Facility was supported by NIH (NS047101), SJ, JJ, JK were partially supported by the National Sustainability Program I, project number LO1609 (Czech Ministry of Education, Youth and Sports), and RVO: 67985904. AM was partially supported by NIH (PO1-HL066941). JB is also supported by NIH grants (CA157885 and CA128893). ARM is supported by grants from the California Institute for Regenerative Medicine (CIRM) TR2-01814 and TR4-06747, the National Institutes of Health through the R21MH107771, R01MH094753, U19MH107367 and a NARSAD Independent Investigator Grant to A.R.M.

Author contributions: J.S., C.C., S.M., T.K., D.D., M.H-P., J.K. performed in vitro experiments; C.B., O.P. performed in vitro electrophysiology experiments; A.M. developed and characterized HIV1 vectors; S.P.D., T.D.G., S.L.P. performed and analyzed mRNA sequencing experiment; M.N., P.X.Ch. performed immunofluorescence staining and microscopy imaging; A.N.G., J.K., T.T., K.K., T.Y., S.J., J.J., J.C., E.C. performed in vivo cell grafting; Ch.S.H. performed SLA genotyping and contributed to writing the paper; A.J.T., F.H.G., J.B., K.Y., A.M., contributed to design and writing the paper; M.M. design the experiment, provided funding and wrote the paper.

Competing interests:

Martin Marsala is the scientific founder of Neurgain Technologies, Inc. and has an equity interest in the company. In addition, Martin Marsala serves as a consultant to Neurgain Technologies, Inc., and receives compensation for these services. The terms of this arrangement have been reviewed and approved by the University of California, San Diego in accordance with its conflict of interest policies. Alysson Muotri is a co-founder and has equity interest in TISMOO, a company dedicated to genetic analysis focusing on therapeutic applications customized for autism spectrum disorder and other neurological disorders with genetic origins. The terms of this arrangement have been reviewed and approved by the University of California San Diego in accordance with its conflict of interest policies. All other authors declare that no competing interest(s) exist.

Data and materials availability:

Requests for the porcine iPSCs and the porcine mRNA sequencing data should be directed to M.Marsala (mmarsala@ucsd.edu) and Samuel L. Pfaff (pfaff@salk.edu) and will be supplied upon completion of a material transfer agreement, which will contain a description of the proposed research using the materials and the data.

Figure legends:

Figure 1. In vitro-differentiated porcine iPSCs-derived neural precursors give rise to functional neurons. (A) Schematic diagram of the experimental time line and design in vitro and in vivo. (B-H) Cultured fibroblasts (B) formed colonies of pluripotent cells (Pluri. Colonies) at 10 days after infection (C, D) and expressed pluripotent markers including KLF4 (E), SOX2 (F), OCT4 (G) and Nanog (H). (I) Established iPSCs-derived embryoid bodies cultured in non-attachment culture flasks. (J) Hematoxylin and Eosin staining of mouse testes at 6 weeks after injection of iPS cells suspended in

matrigel. Development of mature teratoma with identifiable all 3 germ layer derivatives including neural tube rosettes (1. ectoderm-red arrows; upper insert), smooth muscle (2. mesoderm-red arrows; middle insert) and gut cuboidal epithelium with goblet cells (3. endoderm-red arrows; lower insert) can be seen. **(K, L)** NPCs colonies were manually harvested from the periphery of attached and induced embryoid bodies/neural rosettes (K) and further expanded (L). **(M-P)** Long-term expanded NPCs show expression of markers typical of neural precursors including SOX2 (M), PAX6 (N, P), SOX1 (O) and Nestin (N,O). **(R-U)** Staining of induced SYN-EGFP-NPCs (R) with neuronal markers DCX (S, T), NeuN (S) and Tuj1 (U) was seen. A sub-population of DCX⁺ neurons was GABA-immunoreactive (T). **(V)** Fluo-4 AM-loaded, two month-induced NPCs showing spontaneous intracellular calcium oscillation in axons (1, 1') and neuronal soma (2, 2' and 3, 3'). Scale bars: J-500 μm ; M-10 μm ; N-15 μm ; O-10 μm ; S, T, U-10 μm).

Figure 2. Intrastriatal grafting of iPSCs-NPCs in immunodeficient rats is associated with robust neuronal differentiation and appearance of mature and functional grafted neurons at 7-10 months after grafting. **(A, B)** Schematic representation of the experimental time line and design. **(C, D)** Action potential firing (C) (evoked by a depolarizing step of current of 75 pA for 500 ms from resting potential in current-clamp at 0 pA), and voltage gated sodium and potassium currents (D) (evoked by a series of depolarizing steps of 5 mV in voltage-clamp at -70 mV) in grafted SYN-EGFP neurons. **(E, F)** Staining of paraformaldehyde-fixed SYN-EGFP⁺ grafted striatal section with NeuN (E) and NSE (F) antibodies. **(G-I)** Immunofluorescence staining with SYN, NeuN, VGAT and gephyrin antibody (I) in the core of EGFP⁺ graft (G, I) and in areas distant from the graft core (medial region of NPCs-grafted striatum), (H). **(Scale Bars:** E- 50 μm ; F- 10 μm ; G-5 μm ; H, I-20 μm).

Figure 3. iPSCs-NPCs grafted into striata of immunodeficient rats acquire genetic signature of mature porcine CNS at 10 months after grafting. **(A-D)** Schematic representation of the experimental time line and design. **(E)** Analysis and pre-processing of mixed-species RNA-seq reads. **(F)** t-distributed stochastic neighbor embedding (t-SNE) plot showing the degree of correlation in gene expression profiles between the indicated samples.

Figure 4. Spinally-grafted iPSCs-NPCs show long-term survival and neuronal and glial differentiation in syngeneic recipient in the absence of immunosuppression.

(A) Immunofluorescence staining showing EGFP fluorescence in the core of the graft. **(B, C)** Immunofluorescence staining showing NF and GFAP-stained processes in the same areas as in "A". **(D-F)** Staining with DCX (D) NeuN (E) and NSE (F) in EGFP⁺ grafts. **(G-I)** Immunofluorescence

staining showing EGFP/NF+ neurites, in areas cranial and caudal to the borders of the graft. **(J, K)** Co-staining of SYN-EGFP+ grafts with VGAT and gephrin (Gephr) antibodies in the core of the graft. **(Scale Bars:** A-30 μm ; B-125 μm ; C-10 μm ; D-40 μm ; E, F-35 μm ; G, H, I-50 μm ; J, K-20 μm).

Figure 5. Syngeneic iPSCs-NPCs recipients show no humoral immunity against grafted cells at 3 months after cell transplantation in the absence of immunosuppression.

(A) Schematic diagram of the development of *in vivo/ex vivo* staining protocol to detect the presence of circulating antibodies against grafted iPSCs-NPCs. **(B-D)** Staining of mature iPSCs-NPCs grafts in rat striatum and rat spinal cord with serum from previously anti-iPSCs-NPCs-immunized pig (B), sera harvested from naive non-immunized pig (C) or with sera from syngeneic iPSCs-NPCs-grafted pigs (n=3) (D) 3 months after grafting. **(Scale Bars:** B, C, D-40 μm).

Figure 6. Spinally-grafted iPSCs-NPCs show long-term survival and neuronal and glial differentiation in allogeneic spinally-injured pigs with transient immunosuppression.

(A) Schematic diagram of experimental design. **(B-F)** Co-staining of EGFP+ grafts with NeuN, synaptophysin and GFAP antibodies. **(G)** Co-staining with NF and NeuN antibodies in the core of the graft. **(H)** Co-staining of DCX, EGFP and NSE in the core of the graft. **(I)** Confocal microscopy image of SYN, VGAT puncta on EGFP+ grafted neurons. **(J)** Staining of EGFP+ grafted neuron with VGAT and Gephr antibody. **(K)** Co-staining with HOMER and NF antibodies of EGFP+ grafted neurons (white arrows indicate HOMER+ puncta on neuronal soma or axons of EGFP+ neurons). **(L-N)** Confocal images of double-labeled EGFP+/OLIG2+ oligodendrocytes and EGFP+/GFAP+ astrocytes. **(O, P)** Staining of mature iPSCs-NPCs-EGFP+ grafts in rat striata with sera from anti-iPSCs-NPCs-immunized pigs (O) or with sera from iPSCs-NPCs grafted-transiently-immunosuppressed allogeneic pig (n=3) (P). **(Scale Bars:** B-300 μm ; C-500 μm ; D, E, F-60 μm ; G-250 μm ; H-60 μm ; I-10 μm ; J-5 μm ; K- 10 μm ; L, N-10 μm ; O, P-40 μm).

Figure 7. Transient immunosuppression (4 weeks) supports long-term graft survival and is associated with progressive decrease in spinal regional inflammatory response in iPSCs-NPCs-grafted spinally-injured allogeneic pig.

(A-C) Immunofluorescence staining for MHC-II and EGFP around cell injection needle tract in syngeneic pigs (A; n=3) and in allogeneic continuously-immunosuppressed (B; n=3) or transiently immunosuppressed (C; n=3) spinally-injured pigs 4 weeks or 3.5 months after cell grafting. **(D-F)** Immunofluorescence staining for Iba-1 and EGFP around cell injection needle tract in syngeneic pigs (D) and in allogeneic continuously-immunosuppressed (E) or

transiently immunosuppressed (F) spinally-injured pigs 4 weeks or 3.5 months after cell grafting. **(G-I)** Immunofluorescence staining for CD45, CD8 and EGFP around cell injection needle tract in syngeneic pigs (G) and in allogeneic continuously-immunosuppressed (H) or transiently immunosuppressed (I) spinally-injured pigs 4 weeks or 3.5 months after cell grafting. **(J)** Colocalization of MHC-II with Iba-1 in the core of the graft. **(K, L)** Quantitative analysis of CD45+ and CD8+ leukocytes in EGFP+ grafts and in surrounding host tissue (Student's T-test; * $P < 0.05$) **(Scale Bars:** A, B, C, G, H, I-300 μm ; D, E, F-20 μm ; J-10 μm).

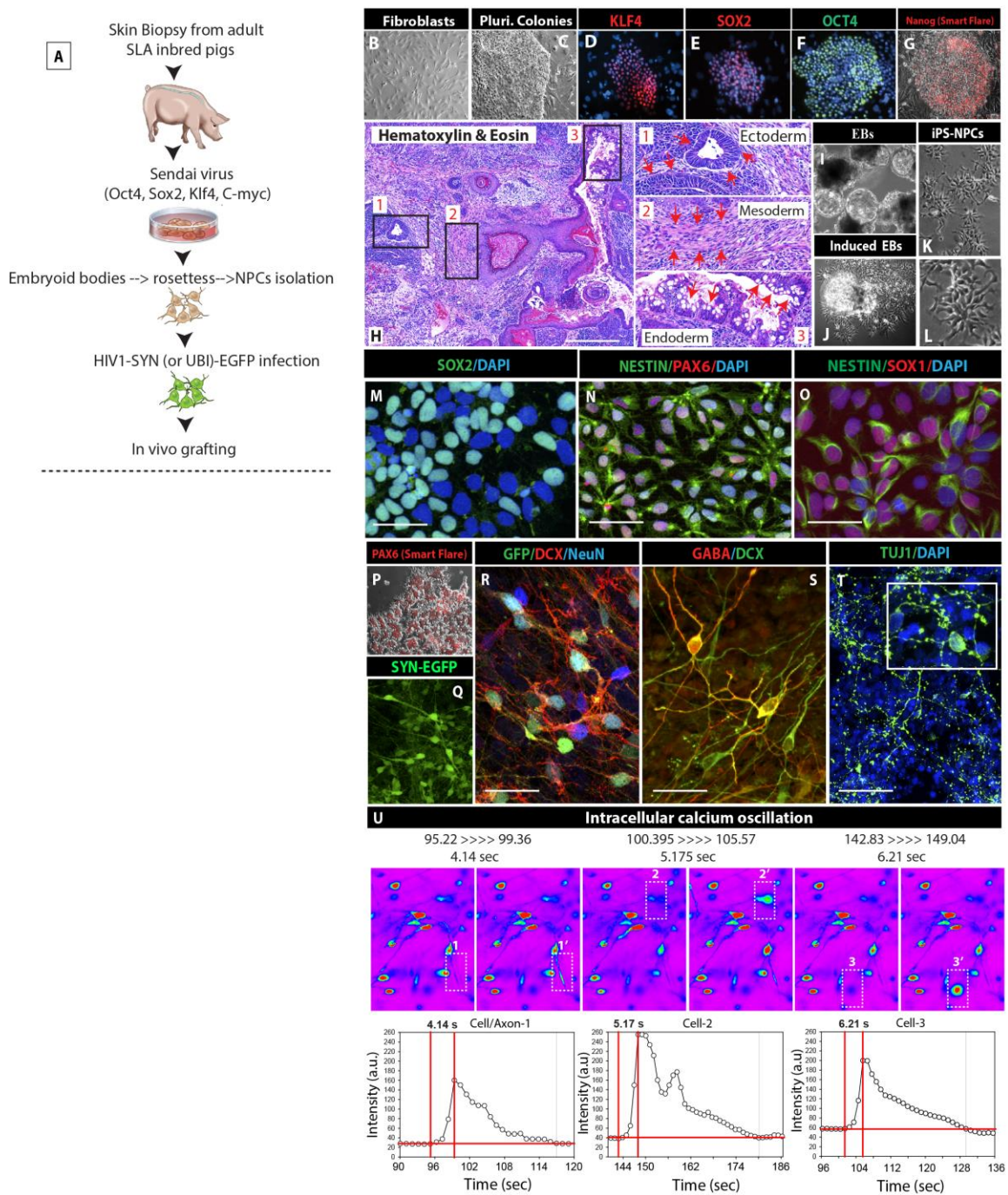


Fig.1 A-U

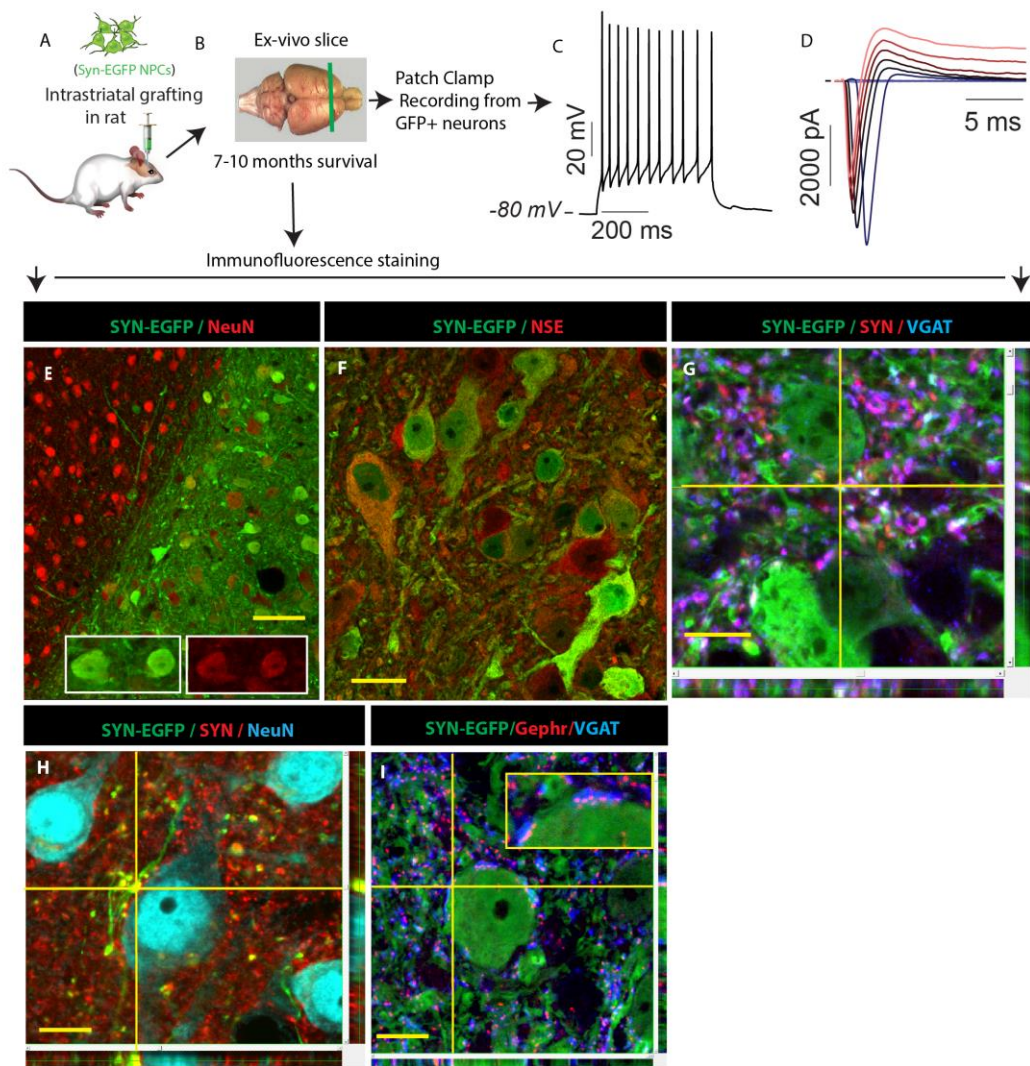


Fig.2 A-I

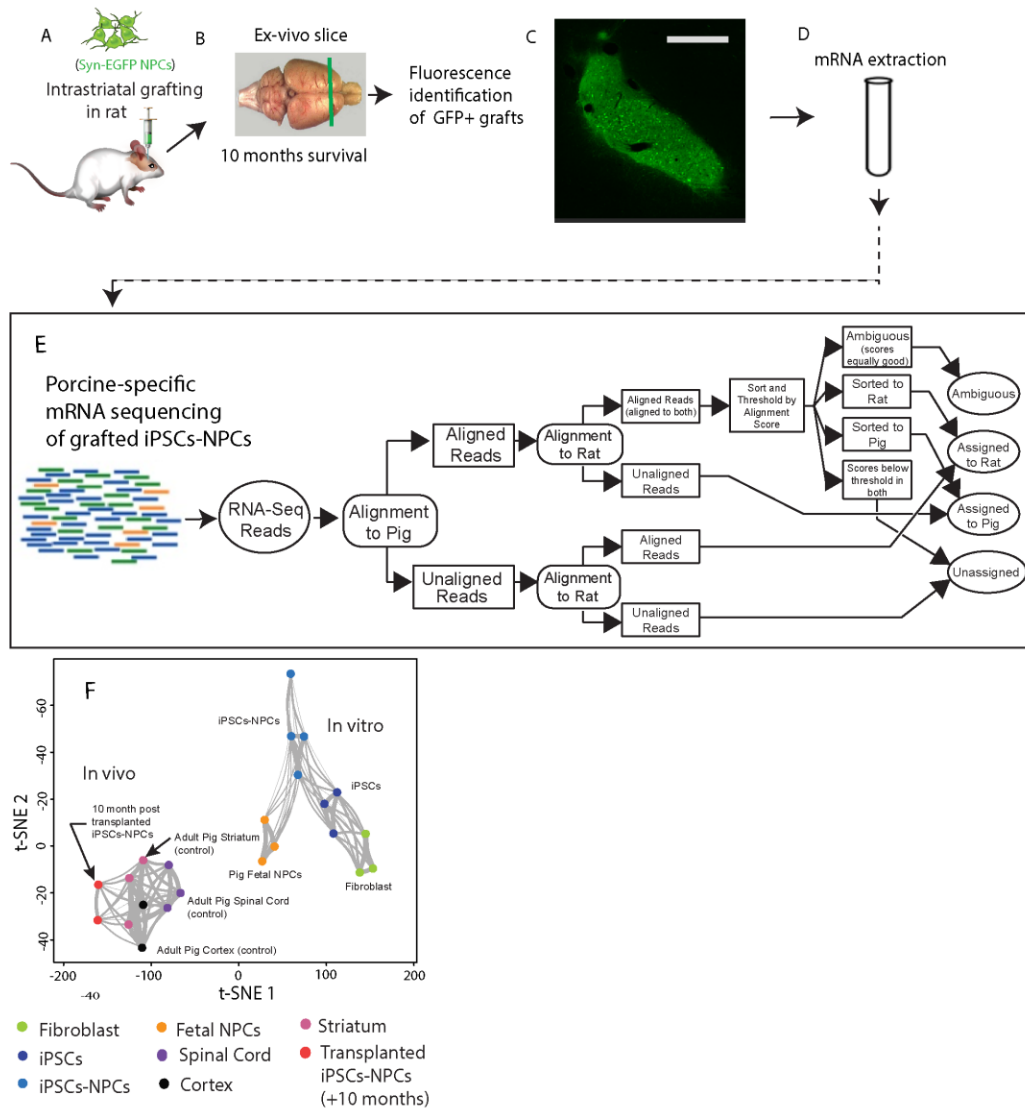


Fig.3 A-F

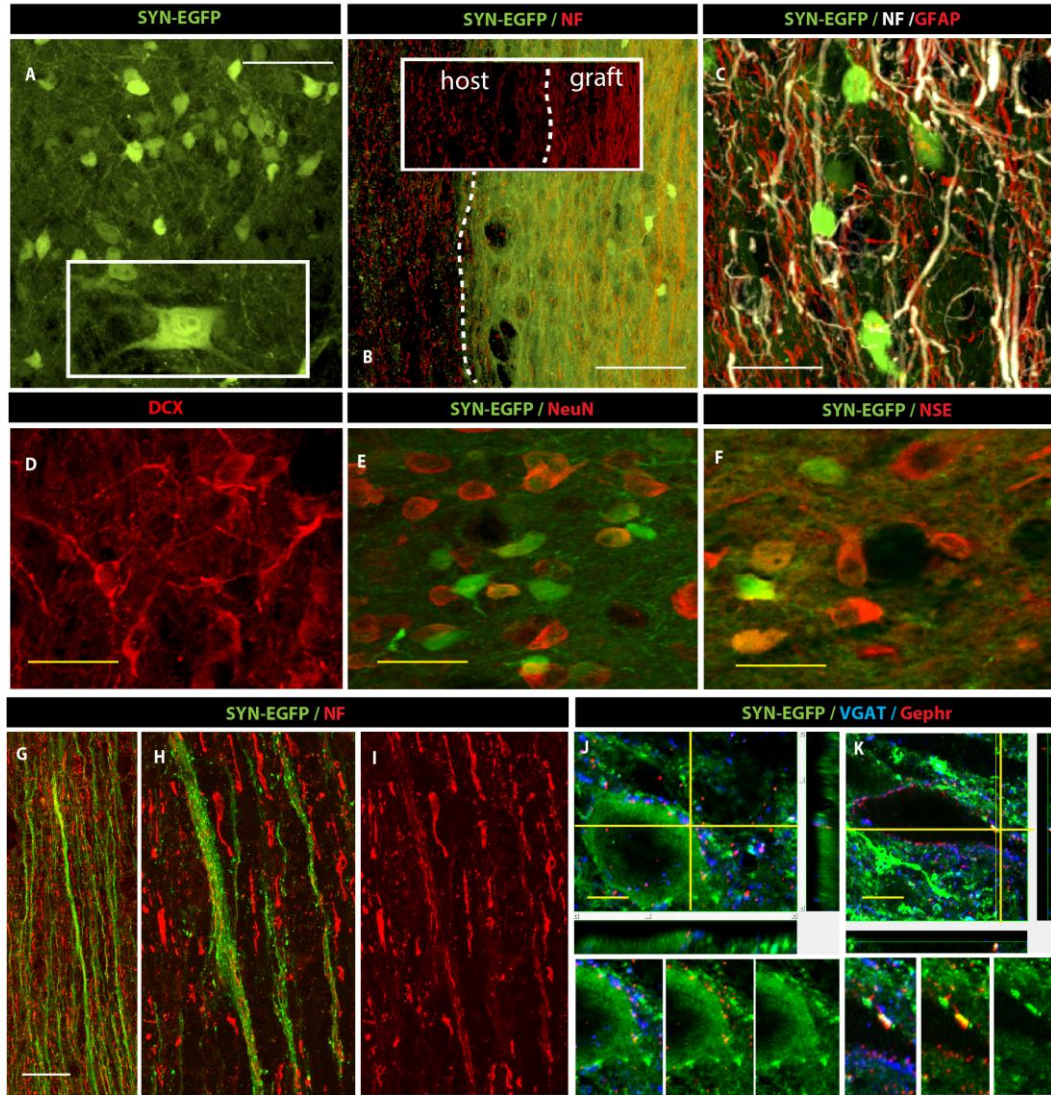


Fig.4 A-K

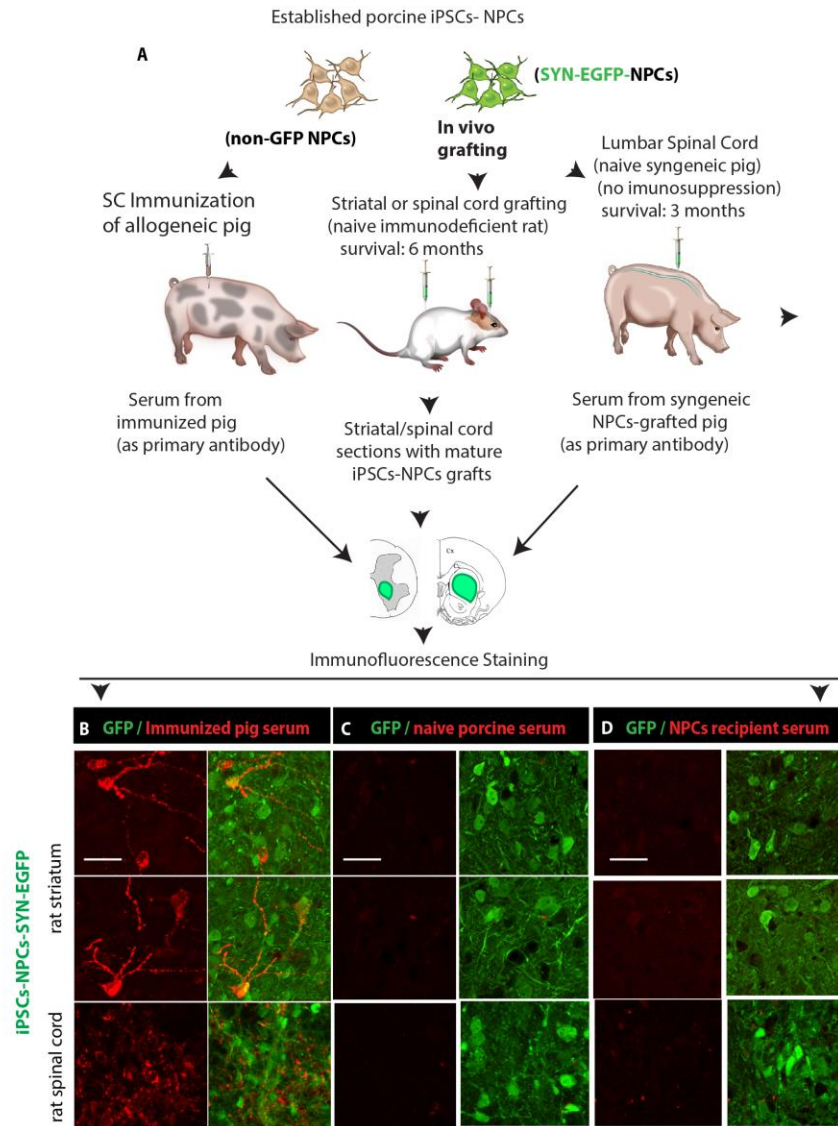


Fig.5 A-D

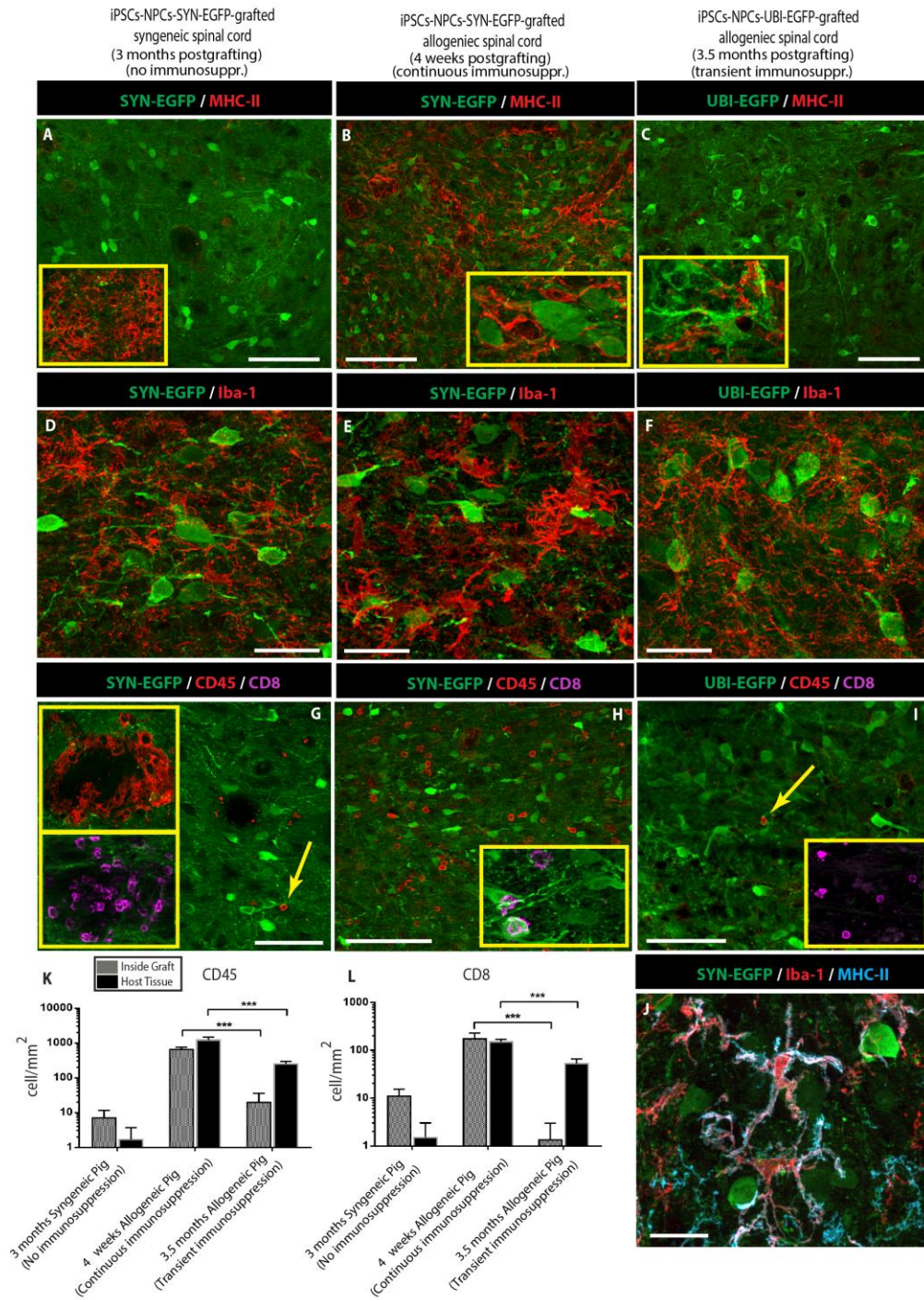


Fig.7 A- L